water

MDPI

Article

Risk Colored Snake (RCS): An Innovative Method for Evaluating Flooding Risk of Linear Hydraulic Infrastructures

José-Luis Molina [1], Santiago Zazo [1,*], Fernando Espejo [1], Carmen Patino-Alonso [2], Irene Blanco-Gutiérrez [3,4] and Domingo Zarzo [5]

[1] Ingeniería y Gestión del Agua (IGA) Research Group, High Polytechnic School of Engineering, University of Salamanca, Av. de los Hornos Caleros, 50, 05003 Ávila, Spain; jlmolina@usal.es (J.-L.M.); espejo@usal.es (F.E.)
[2] Ingeniería y Gestión del Agua (IGA) Research Group, Department of Statistics, Campus Miguel de Unamuno, University of Salamanca, C/Alfonso X El Sabio s/n, 37007 Salamanca, Spain; carpatino@usal.es
[3] Centro de Estudios e Investigación para la Gestión de Riesgos Agrarios y. Medioambientales (CEIGRAM), Universidad Politécnica de Madrid, Senda del Rey 13, 28040 Madrid, Spain; irene.blanco@upm.es
[4] Department of Agricultural Economics, Statistics and Business Management, Escuela Técnica Superior de Ingeniería Agronómica, Alimentaria y de Biosistemas (ETSIAAB), Campus Ciudad Universitaria, Universidad Politécnica de Madrid, Av. Puerta de Hierro 2-4, 28040 Madrid, Spain
[5] Innovation and Strategic Projects, Sacyr Agua, Paseo de la Castellana, 83-85, 28046 Madrid, Spain; dzarzo@sacyr.com
* Correspondence: szazo@usal.es

Abstract: Floods are probably the most hazardous global natural event as well as the main cause of human losses and economic damage. They are often hard to predict, but their consequences may be reduced by taking the right precautions. In this sense, hydraulic infrastructures, such as dams, are generally the most widely used management elements to significantly mitigate this natural risk. However, others, such as linear ones, mainly ditches and canals, can both in themselves be potentially active risk-generating factors and vectors of flooding risk propagation. The aim of this research is to develop an accurate and detailed technique for assessing the intrinsic risk of these infrastructures due to flood events. This is performed based on two key factors: the proximity to urban areas and the water level reached in the infrastructures. Consequently, this research is developed through a double geomatic and hydraulic component organized into four steps: topological processing, parameter computation, risk calculation, and development of the Risk Colored Snake (RCS) technique. This was successfully applied to the network of irrigation ditches of Almoradí in Alicante (Spain), which is characterized by a high exposure level to flood hazards. RCS is a valuable tool to easily assess the potential risk of each section of the linear hydraulic infrastructures. By means of color-coding RCS, it is simpler for the end user to quickly detect potentially problematic locations in an accurate and detailed manner.

Keywords: risk colored snake; flooding; hydraulic infrastructures; risk assessment; mapping algebra

Citation: Molina, J.-L.; Zazo, S.; Espejo, F.; Patino-Alonso, C.; Blanco-Gutiérrez, I.; Zarzo, D. Risk Colored Snake (RCS): An Innovative Method for Evaluating Flooding Risk of Linear Hydraulic Infrastructures. *Water* **2024**, *16*, 506. https://doi.org/10.3390/w16030506

Academic Editor: Reza Derakhshani

Received: 10 January 2024
Revised: 2 February 2024
Accepted: 4 February 2024
Published: 5 February 2024

1. Introduction

Damage caused by natural disasters is a constant threat to the population, largely due to the uncertainty involved. Good planning, readiness, and a proper risk assessment, together with adequate decision-making, can increase safety and reduce damage. This involves knowing the hazards and risks of each territory. Furthermore, hydraulic infrastructures, especially linear ones such as canals and irrigation ditches, are also vulnerable to natural disasters such as floods. The impacts can go far beyond the calculated spatiotemporal physical affected frame. This is due to linear infrastructures themselves being susceptible to propagating the induced failure through linear hydraulic infrastructures [1–4]. This is normally a consequence of necessary terrain modification. Usually, those infrastructures are used for agricultural purposes.

Conversely, due to global warming, flood episodes are increasing [5]. In this sense, it is predicted that by 2050 the phenomena will become more frequent [6]. That makes it essential to have prevention and risk assessment plans in place. This mainly involves knowing which areas are most likely to be at risk [7]. According to the Centre for Research on the Epidemiology of Disasters (CRED) and the United Nations Office for Disaster Risk Reduction (UNISD), floods have caused the most disasters in the period 1998–2017, accounting for 43.4% of recorded disasters and 23% of total economic losses [7]. In Europe, the average annual damage due to floods in the period 2000–2012 was EUR 4.2 billion, and the forecast is that by 2050 this will increase to EUR 23.5 billion [7]. In Spain, according to the Insurance Compensation Consortium (the Spanish public reinsurer), in the period 1971–2021, almost 46% of the claims processed were due to floods and accounted for 64% of the total compensation [8].

Traditionally, flood risk is understood as the probability of expected losses occurring in the event of a flood. This approach is based on four (4) key concepts: (i) susceptibility, (ii) vulnerability, (iii) hazard, and (iv) level of exposure [9–11]. Susceptibility is a concept related to the occurrence of certain phenomena in an area. Vulnerability refers to the ability of each element to cope with the risk. Hazard is related to the magnitude, severity, and frequency with which the event manifests itself. Specifically, in the event of floods, a hazard corresponds to the depth, velocity, and extent of the water surface [12]. Finally, exposure encompasses the properties that may be damaged by the flood event (risk elements), which depends mainly on their distance to the risk source [12]. Therefore, conceptually, the risk level is determined as a result of multiplying hazard, exposure, and vulnerability [9,10]. In this manner, once risks have been analyzed, the level of risk is assessed and thresholded, and preventive measures may finally be implemented.

It is possible to create interactive maps, created by multi-criteria analysis, in which the most vulnerable points with the greatest possibility of suffering flood damage can be identified. For this purpose, cartography has been and still is a highly effective tool for showing the results of natural risk analysis [13]. Likewise, cartography serves both to raise public awareness and to plan actions in case of emergency [14]. In this sense, the identification of risk at points of special importance is key, and hydraulic risk maps are the baseline for land use and emergency planning [15,16].

Conversely, flood risk mapping focuses on showing the effects that a given flow would have on a territory, encompassing all the elements on the ground [17]. However, these flood events may involve flow rates greater than the transport capacities of linear infrastructures. These infrastructures usually initiate from the main rivers in the area. In the case of a river level rise due to a hydrological event, the amount of water flowing through the canals increases and they may behave like active elements of risk propagation. Thus, the network of irrigation ditches and irrigation channels can act as a vector of flow [18]. This is especially important if the cleaning and maintenance norms for their correct drainage are not followed [19]. In these cases, linear infrastructures reverse their natural flow direction and become risk generating elements around them [20,21]. Generally, the overflow in irrigation ditches that produces flooding and runs inside towns must be intercepted before reaching the dam to divert it and provide continuity without affecting the urban areas [22].

In this work, the study areas comprise hydraulic infrastructures largely used for irrigation purposes. Affected areas often need public support to repair damaged agricultural infrastructures and help to compensate farmers for their losses (loss of production and even death of trees, cattle, and crops) [23]. In many cases, this results in expensive compensation based on complex insurance methods [24]. Furthermore, linear infrastructures are considered in themselves as potentially active risk-generating and risk propagation vectors to flooding. This implies an infrastructure-based approach rather than the classical territorial flooding approach.

The aim of this research is to develop an accurate and detailed technique for assessing the intrinsic risk of these infrastructures due to flood events. This is performed based on two key factors: (i) the proximity to urban areas, given that these areas are more susceptible to damage from overflowing, and (ii) the water level in the infrastructures (depth). This challenge is developed through double geomatic and hydraulic components. This manuscript is organized into four steps: topological processing, parameter computation, risk calculation, and development of an innovative Risk Colored Snake (RCS) technique. The result is a map of linear infrastructures categorized by color coding according to the potential risk of each section. Through color coding, RCS increases the risk visualization ability and makes it simpler for the end user to quickly detect potentially problematic locations in an accurate and detailed manner. This analysis can provide valuable information to water planners and managers, as well as civil protection agencies. This also improves prevention and enables more effective flood management strategies tailored to local conditions.

2. Materials

2.1. Case Study

In Spain, the greatest flood damage, in absolute terms, is concentrated in the Mediterranean area, especially in the provinces of Alicante, Valencia, and Murcia [12]. These areas are densely populated regions, with great economic dynamism, also due to the great influence of the agricultural sector, and where precipitation events are characterized by high intensity and short duration. Thus, this research is focused on the network of irrigation ditches of Almoradí, located in Vega Baja del Segura region in the province of Alicante (Valencian Community, Alicante province, Spain; Figure 1). This area covers an area of 957.28 km^2 (16.46% of the total area of the province). Within the region, the farming area (approximately 183 km^2) is supplied with water diverted from the Segura River through irrigation channels or ditches that distribute the water through the farmland and make up what is known as the "living water network".

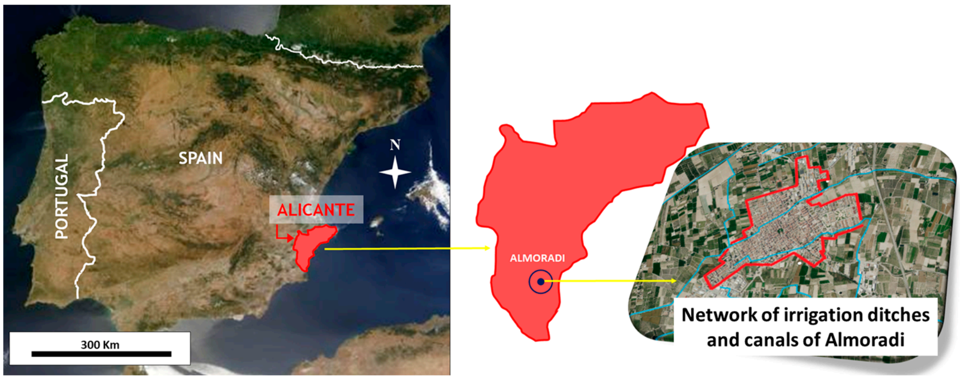

Figure 1. Case study situation, Almoradí (Alicante, Spain). Source: Spatial Data Infrastructure of Spain; open access data according to INSPIRE European Union Directive. Specification Web Map Tile Service (WMTS) from Open Geospatial Consortium, Inc. (OGC) Arlington, VA 22201, USA. Digital orthoimages from National Plan for Territory Observation. Coordinate Reference System: EPSG: 25830; Almoradi: 30S—688384 4221429.

Almoradí is placed on a large alluvial plain of the Segura River and is part of the "Vega Baja" county. Due to its flat orography and that the Segura River borders the town of Almoradí, the susceptibility of agricultural land and peri-urban areas to flood damage is relevant, especially in the case of extreme events.

The Vega Baja of the Segura River has an extensive record of floods, with data from the twelfth century to the present day [25]. From the twentieth century until now, more than one hundred episodes of flooding have been recorded in this area. Among the most important episodes in Almoradí are the flows of 1947 and 1948, when torrential rains caused the Segura River to overflow. In 1987, the catastrophic results of floods led to the emergency approval of the Segura River Basin Flood Control Plan [26]. Although this action included interventions such as the creation of dams, canals, and wadis, the fact is that the action was mainly focused on canalization of the Segura River from its entrance in Orihuela to Guardamar del Segura (roughly 40 km). Meanders were removed to facilitate the slope and the velocity of the water [27]. After these actions, the first overflow of the Segura River occurred in 2016. In that same year, it was observed that the canalization of the river could cause similar effects to those produced in the 1987 flood. Basically, it was concluded that the canalization generated a false sense of security [28] that led to the construction of houses in flood zones. Three years later, in 2019, the last major flood occurred in this area, which showed that structural solutions are not sufficient to prevent this type of catastrophe [29]. During this episode, Almoradí and other adjoining localities were left without water supply. The river canalization was broken in Almoradí, Benejúzar, and Algorfa. Specifically, in Almoradí, two pipes were broken, which caused the flooding of the industrial estate and downstream towns and the loss of citrus and horticultural crop production. Furthermore, the water level in this area exceeded the water level of the 1987 floods, resulting in the worst event of this kind in the history of agricultural insurance. Thirty percent of the harvest was lost and economic losses in the agricultural sector amounted to more than EUR 6 million (about EUR 3000/ha in citrus, the most affected crops), with EUR 3.5 million in agricultural insurance indemnities [30]. In this episode, the combination of extreme rainfall events and flooding produced in total damages of approximately EUR 1319 million, including agricultural losses, of which EUR 475 million was compensation for personal damages [12,31].

Among all the irrigation ditches that make up the network of Almoradí and its surroundings, two are of special importance for the risk analysis, given their proximity to urban areas: the Major Ditch of Almoradí and the Calvario Ditch (Figure 2). Both cross the urban area in whole or in part and are the main object of the case study. The Major Ditch of Almoradí runs almost parallel to the river and has a high branching. Its length is 6730 m, along which irrigates an area of 2062 hectares [32]. The distribution of living waters is made up of 5 minor irrigation ditches, 84 lines, and more than 200 small irrigation ditches [33].

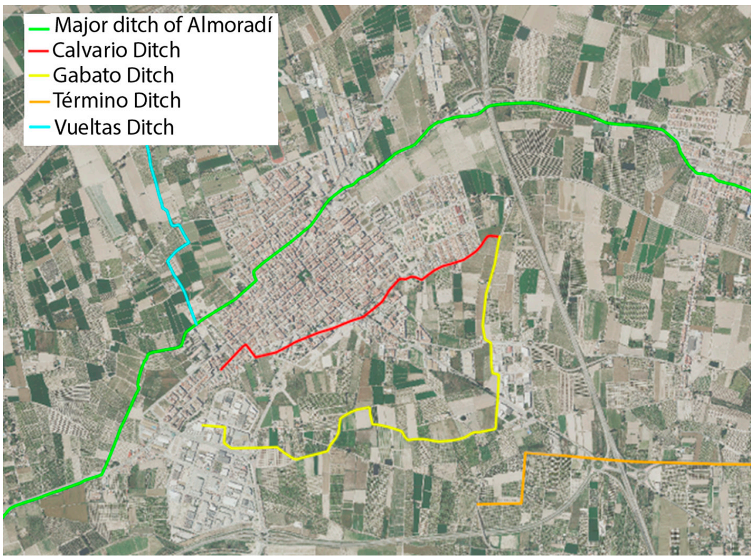

Figure 2. Network irrigation ditches of Almoradí (edited by the authors). Source: Spatial Data Infrastructure of Spain; open access data according to INSPIRE European Union Directive. Specification WMTS from Open Geospatial Consortium, Inc. (OGC). Digital orthoimage from National Plan for Territory Observation.

2.2. Flood Hazards Cartography Considered

In Spain, several flood cartographies are available, both at the national and regional level; in this case, two of them stand out: the National Flood Zone Mapping System, Spanish acronym SNZCI at national scale, and the Sectoral Territorial Action Plan on

Flood Risk Prevention in the Valencian Community, PATRICOVA (Spanish acronym), specific to Valencian Community. Both offer flood risk maps but with differences between them. SNZCI categorizes the risk in four groups (population, economic activity, points of special interest, and areas of environmental importance), while PATRICOVA does so in six. Similarly, SNZCI establishes three hazard scenarios, and, in contrast, PATRICOVA defines six, highlighted that the latter considers geomorphological hazards, although it does not represent them in the cartography. Indeed, when geomorphological hazards are considered, the total number of affected structures is much higher. This characteristic should be represented in any cartography to be totally truthful, although to date neither SNZCI nor PATRICOVA incorporate it [29]. Figure 3 shows the PATRICOVA flood risk assessment.

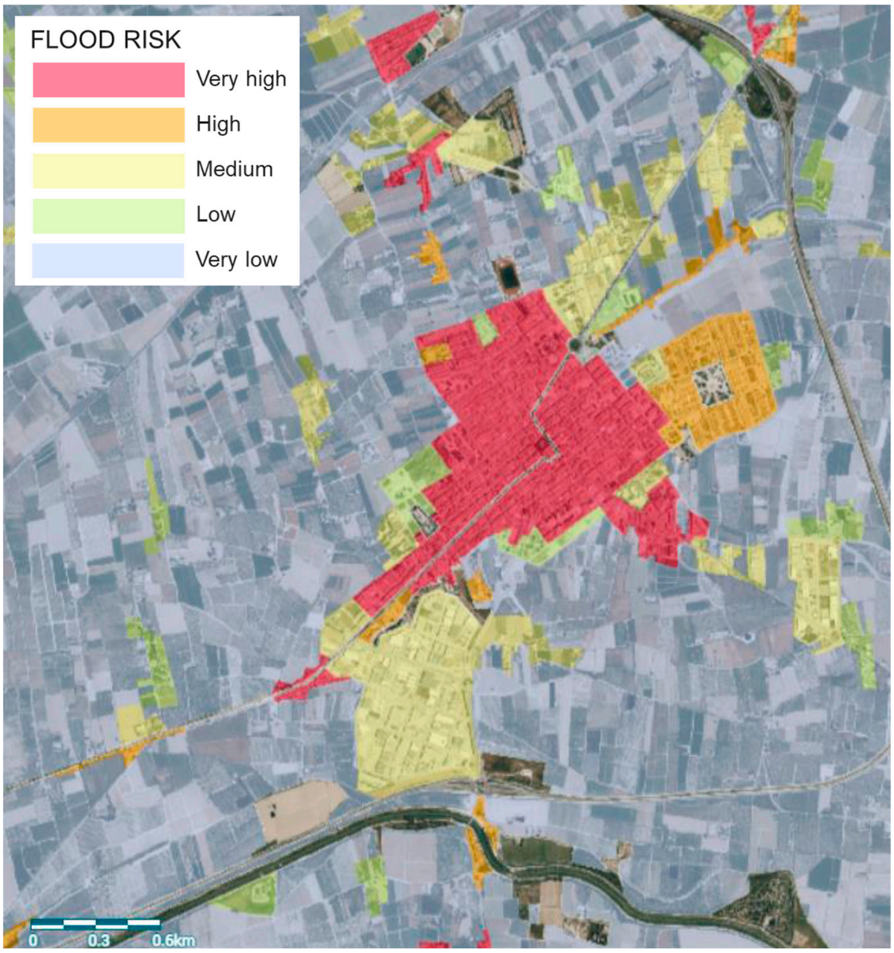

Figure 3. PATRICOVA flood risk assessment.

Due to the more detailed hazard shown in PATRICOVA, this one has been used to assess the risk flood of the linear infrastructures. On the other hand, this cartography is based on the events' frequency and the floods' depth. For this reason, the height of the flood (depth) is a key parameter in this research. According to PATRICOVA [34], the entire study area is defined as hazard scenario 2, with an average flood frequency of 100 years and a depth higher than 0.8 m.

2.3. Data Acquisition

Data acquisition consists mainly of downloading the necessary layers of geospatial information. Specifically, three layers of information are needed: (i) information related to ditches and canals in the study area, (ii) urban area boundaries, and (iii) flood map of the area. The first two layers are vectorial, while the last one is a raster layer of 1 m × 1 m resolution. Regarding the vector layers, both are in shapefile format [35]. In this sense, the difference between both vector layers is that the one corresponding to canals and irrigation ditches contains linear geometries while the one corresponding to urban area boundaries contains polygonal geometries. Additional data contained in the shapefiles refer to the identification of infrastructure, location, population, type of construction, etc.

The raster information of the flooding layer is in GeoTIFF format, which is an extension of the popular TIFF format, to support a geodetically sound raster data georeferencing capability. The geographic content supported in the GeoTIFF tag structure includes its cartographic projection, data, ground pixel dimension, and other geographic variables [36]. Taking this into account, each pixel of the raster file contains information about the maximum depth at that point. These data are freely provided through National Center for Geographic Information according to INSPIRE Directive [37]. They are based on hydraulic simulations according to a particular return period (in this case, 100 years as PATRICOVA), in which the terrain is obtained through LIDAR (Laser Imaging Detection and Ranging) technology, from the National Plan of Aerial Orthophotography of Spain. These geometrical data have a spatial resolution up to 2 points/m^2, with an altimetric accuracy higher than 0.20 m (RMSE $\leq$ 0.20 m) [38].

2.4. Software and Tools

A Windows operating system with a 64-bit Intel Core i7 processor and 12 Gb RAM memory was used. The geographic and spatial operations QGIS 3.22 software was used because it is one of the most popular open-source GISs, with a growing user base and increasing importance in the educational and research sector [39]. QGIS allows to create, edit, and operate with different spatial data and cartography and is cross-platform.

The rest of the necessary in-house developments were implemented using the Python 3 programming language. Python is free, cross-platform, and easy to learn or read, which facilitates the conversion of ideas to code [40]. It has efficient high-level data structures and a simple but effective object-oriented programming system [41].

One of the major advantages of Python is that it includes libraries from a wide variety of disciplines that can be included in projects. This is the case with PyQGIS [42], GRASS [43], and PyQt5 [44] libraries used for the development of the tool.

3. Methodology

This research has a double fluvial hydraulic and geomatics component articulated in four main sequential steps: topological processing, parameter calculation, risk calculation, and generation of the Risk Colored Snake (RCS; Figure 4).

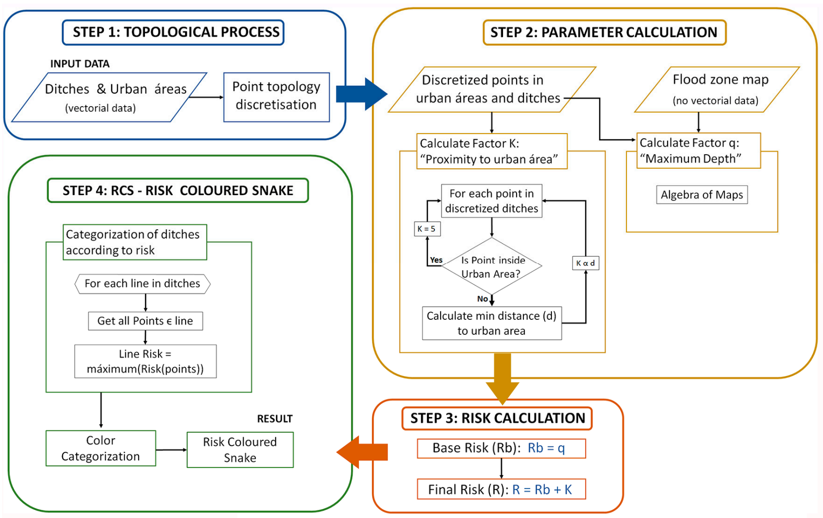

Figure 4. Proposed methodology.

3.1. Step 1: Topological Process

In this initial step, the necessary topological operations are performed to adapt the input data to the data required by the algorithms. All line or polygon topologies are converted to points by means of a distance-based discretization. This discretization distance has been established by trial and error at 20 m for irrigation ditches and 1 m for urban areas.

3.2. Step 2: Parameter Calculation

Two essential parameters for determining the risk of any infrastructure are calculated: (i) maximum depth ("q" parameter) and (ii) proximity to urban area ("K" parameter).

The maximum depth is obtained by map algebra process. Thus, for each discretized point in Step 1, the value of the maximum depth contained in the flood map (raster format) is obtained. The result is stored in a new information field. Finally, the parameter "q" acquires values proportional to the maximum depth (Table 1; "q" parameter).

Table 1. Calculation of "q" parameter based on the depth of each point and "K" parameter depending on the distance to urban areas. Note: the closer to the urban area, the greater the value. If the point is inside the urban area, the "K" value is the maximum.

"q" Parameter		**"K" Parameter**	
Depth [1]	**"q" Value**	**Urban Area Distance (d [1])**	**"K" Value**
Depth = 0	0	$d \geq 2000$	1
0 < Depth $\leq$ 0.5	5	$1000 \leq d < 2000$	2
0.5 < Depth $\leq$ 1.0	10	$500 \leq d < 1000$	3
1.0 < Depth $\leq$ 1.5	15	$100 \leq d < 500$	4
Depth > 1.5	20	$0 \leq d < 100$ or urban zone	5

Note: [1] expressed in meters.

In contrast, for the calculation of "K" parameter (proximity to the urban zone), a sequential process consisting of two parts is followed: first, it is checked, using map algebra, if the point is within the urban zone, and, second, the value of "K" parameter is calculated. If the point is within an urban area, the parameter has the maximum value, which is 5. In contrast, if the point is not within any urban area, the minimum distance of the point to the urban area is calculated and the parameter "K" acquires a value proportional to this distance (Table 1; "K" parameter).

Conversely, and according to Milanesi et al. [16] and Cox et al. [45], the risk of drowning in humans is closely related to the position of the head of children and adults in relation to the flooding depth. In this sense, Cox et al. [45] propose maximum admissible water depths of 1.2 for adults and 0.5 m for children, while Milanesi et al. [16] recommend constraints of 1.4 and 1 m, respectively, for adults and children. For this reason, and applying a unifying criterion, the thresholding of the parameter "q" has been based on the values recommended in both studies.

3.3. Step 3: Risk Calculation

The risk of each point to hydrological events is determined through two substeps: (i) determination of the base risk (R_{base}) and (ii) determination of the final risk. The base risk considers only the maximum depth and is set in the same way to the "q" parameter. However, the final risk (R) is obtained considering both the maximum depth and the proximity to urban areas. This is expressed as the following:

$$R_{base} = q \quad (1)$$

$$R = R_{base} + K \quad (2)$$

It should be noted that the base risk is additive according to the distance to urban areas to obtain the final value of the risk at each point.

3.4. Step 4: Risk Colored Snakes (RCSs) Generation

In this last and crucial step, for each ditch section, the risk, previously assessed, is assigned. For each section, the assigned risk is the maximum risk of all the points belonging to that section. Then, according to experimental results provided though IGA [46], a color-coding categorization is defined for RCS (Table 2).

Table 2. Color categorization of ditches based on risk.

Risk Value/Assessment		Color Coding
[0, 5)	No risk	
[5, 10)	Low risk	
[10, 15)	Medium risk	
[15, 20)	High risk	
[20, 25]	Extreme risk	

4. Results

Following the methodology described above, the start was set for the vector layers of irrigation ditches and urban areas as well as the raster layer of flood zones (Figure 5a). Once the topological processes of conversion of linear and polygonal entities to points (Figure 5b) have been carried out, the different parameters are calculated.

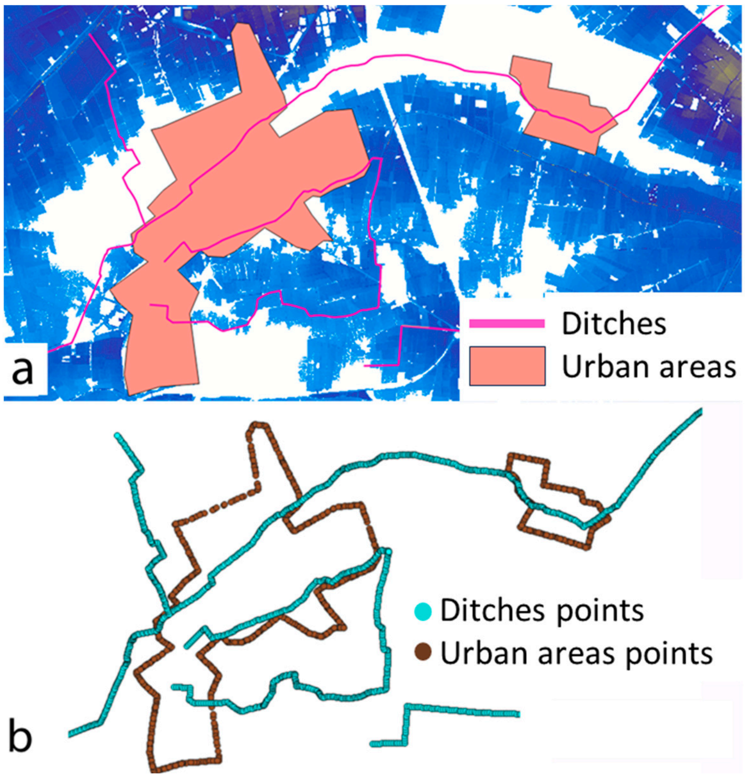

Figure 5. (**a**) Initial data of Almoradí urban area, ditches, and flow map. (**b**) Results of topological conversion from linear and polygonal layers to points.

With the maximum depth extracted from the raster layer, the base risk is calculated according to Table 1. This base risk is used together with the minimum distance of each point to urban areas to obtain the final risk value (Table 3) as shown in Table 1. It is important to note that, if the points are contained within urban areas, the "*K*" parameter is set to the maximum value regardless of the minimum distance since it implies a greater possibility of risk.

Table 3. Sample of points set and calculated parameters. Note: the base risk calculated by means of the depth is shown in the third column. In the last column, the final risk is displayed.

Name	Depth *	R_{base}	Inside Polygon	Distance *	"*K*" Parameter	Risk
1. Major Ditch	0.059	5	False	317.884	4	9
2. Major Ditch	0.957	10	False	103.205	4	14
3. Major Ditch	1.018	15	False	99.184	5	20
4. Calvario Ditch	0.000	0	True	123.631	5	5
5. Calvario Ditch	0.433	5	True	122.179	5	10
6. Calvario Ditch	0.569	10	True	11.617	5	15
7. Calvario Ditch	0.000	0	True	98.146	5	5

Note: * expressed in meters.

The risk is then assigned to the different sections of the irrigation ditches, with the risk of each section being equal to the maximum risk of the points belonging to it (Figure 6a). Finally, the categorization by color is performed (Figure 6b) and the RCS is obtained (Figure 7).

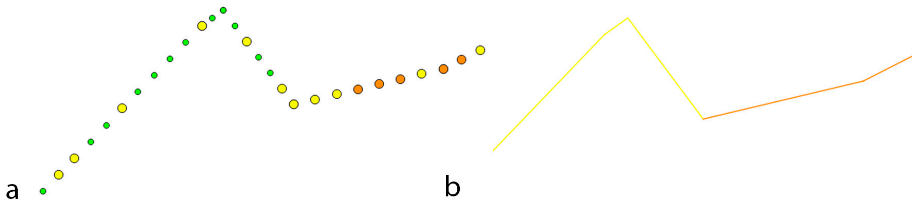

Figure 6. Ditches categorization by risk. (**a**) Points categorized by risk. (**b**) Resultant categorized lines. As can be seen, each section contains several points, so the final risk of the section is the maximum risk of the points. Dots' color represents the flooding risk level.

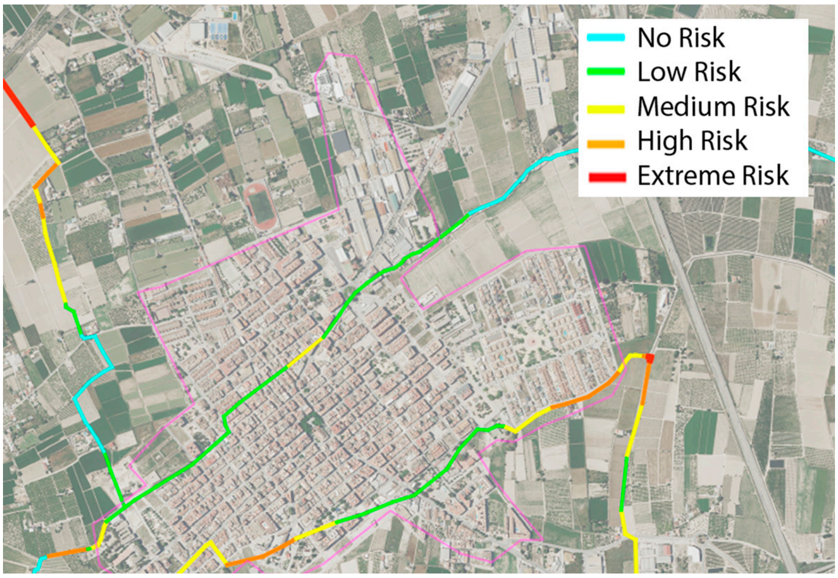

Figure 7. Risk Colored Snake (RCS) resultant from the proposed methodology. Note: urban area limit is represented in magenta color.

4.1. Influence of "K" Parameter

As can be seen in the results, the final risk is determined by the "*K*" parameter (distance to urban areas). This factor increases the value of the base risk, being the maximum increase in one risk level for locations within urban areas. Thus, not only the depth of each area is considered but also its location. The chance that an extreme hydrological event causes damage to facilities is much higher in urban areas than in unpopulated areas. Therefore, the "*K*" parameter always increases the risk value based on the maximum depth.

4.2. Influence of Discretization Distance

One of the most influential factors in the final RCS and its associated risks is the discretization distance of the points, chosen in Step 1 (please see Figure 4). An equidistance of 20 m is set by trial and error. Each ditch section, delimited by the design or construction requirements, is discretized in points so that, if a very large distance is chosen, details will be lost (Figure 8). In contrast, if a very small distance is set, the system will be overloaded with unnecessary operations that will not improve the result.

Figure 8. Influence of the discretization distance in the result. (**a**) Discretization distance is 20 m. (**b**) Discretization distance is 100 m. Some important details are not considered and in consequence the final line risk is lower than real value. Dots' color represents the flooding risk level.

In addition, the resolution of the raster layer with the flooding data must be considered since it will determine the amount of maximum depth data available. For the case study, a 1 m $\times$ 1 m resolution raster is available, which means that there will be one flood data point per square meter. If, on the other hand, a 10 m $\times$ 10 m resolution raster were implemented, consequently, one flood data point per 100 square meters would be expected.

5. Discussion

According to Milanesi et al. [16], the following fundamental requirements are necessary when defining vulnerability criteria are applied to flooding: (i) representing simple processes easily understood by stakeholders, (ii) being easy to use and providing thresholds, with the possibility of adaptation to different flooding environments, and (iii) fitting experimental data reasonably. However, most of the criteria do not match these requirements [47]. The existing regulations provide thresholds for risk assessment, ranging from supranational approaches to more detailed regional and/or local regulations tailored to the realities of their territories.

The risk of flooding on the Spanish Mediterranean coast has continued to increase despite the enormous efforts made to mitigate it [48]. As in many other parts of the world, prevention actions have largely been based on the development of technical and engineering measures. However, recent flood episodes have shown that the construction of hydraulic infrastructures cannot be the only solution to mitigate natural hazards and that the development of integrated risk management plans is also key. In this sense, it has been widely reported that engineering measures derives in a false sense of security, encouraging the occupation of floodplains and increasing the risk exposure [49]. Much less studied is the fact that the construction of irrigation infrastructures can be particularly dangerous in case of floods because they can expand the flooding of the main rivers.

In Almoradí, linear hydraulic infrastructures such as canals and irrigation ditches have been crucial for irrigation development and rural socio-economic progress. In the same way as in other water-scarce regions, these infrastructures have contributed to accelerating the transformation of agricultural production systems, helping the cultivation of more profitable and water-intensive crops (e.g., horticulture) [50]. However, the intensification of agriculture often contributes to modifying the hydrological dynamics of the territory, increasing runoff and flow velocity in the event of heavy rainfall. Therefore, these areas are likely to face increased risk of flooding and concentrate high economic losses. Although the potential damage to agricultural areas is expected to be lower than in urban areas, it has a major impact on decisions concerning flood management [23].

The avoided damage to agriculture is generally acknowledged to be critical because farms are important to the regional economy and food supply. Furthermore, in small rural areas, like Almoradí, agricultural and urban areas are very intermingled, which emphasizes the need to develop fully integrated risk management strategies and coordinated land use and urban planning policies [51]. Therefore, identifying areas where flood risk is potentially significant is key, but this usually focuses on the study of rivers' hydrodynamics, ignoring the network of irrigation ditches.

6. Conclusions

This research has presented a new methodology for categorizing the risk of canals and ditches in the face of hydrological events. This study considers not only the maximum depth, from a human risk perspective ("*q*" parameter), of each point but also the proximity to urban areas. The presented results, in the form of the color-coding RCS, make it easier for the end user to identify and assess potentially dangerous areas immediately. Furthermore, special emphasis has been placed on irrigation infrastructures, which are considered to be potentially dangerous in floods because they expand and propagate the flooding of the main rivers.

Conversely, the potential of RCS methodology can be clearly shown by comparing the risk assessment between Figures 3 and 7. In the first one, the whole urban area is evaluated as "very high flood risk"; however, the detailed analysis offered by RCS allows a much more detailed evaluation. RCS analysis would allow prioritization of structural and non-structural actions to mitigate flood risk in specific areas of the urban area, compared to the general assessment available, based on a traditional approach.

According to the achieved results, the most decisive factor is the proximity to urban areas ("*K*" parameter) as this is where most damage can occur. Thus, an area with a high depth located in an area free of houses may have a lower risk value than an area with a medium depth that runs through the interior of a town. This is the most innovative point of the methodology as the consideration of the proximity to urban areas is an added value for future risk planning.

Another important aspect comprises that, for each section, several points are taken and the risk conditions of each one is assessed, assigning to the line the most unfavorable value of all the points studied. This makes it possible to adapt the results to reality in a more reliable way. However, this approach has a very important conditioning factor: the discretization distance of the points. This factor might condition the result because of the information loss effect or system overloading. In this case, the calculated value by trial and error was 20 m, appropriate for the development of this research.

In the same way, it is necessary to consider the raster resolution and its effect on the result. In this study, a resolution of 1 m $\times$ 1 m has been used, i.e., a maximum depth for each square meter. However, not all raster files have the same resolution, and therefore it is possible to find a raster of 10 m $\times$ 10 m resolution. In this case, it would have a maximum depth per 100 square meters.

Future works will study the influence of the following factors: (i) discretization distance and (ii) spatial resolution of flooding data to the results to determine the suitable combination of both, as well as the automation of their calculation. This research will also be complemented in the future with the analysis of the influence of spatial resolution of raster flooding data in the discretization distance. Other upcoming works comprise, on one hand, the possibility of using other data types for the process, such as vector files, containing the depth information at each point, and, on the other hand, the possibility of making a connection to a database to extract that information.

Finally, this study goes a step further and develops an innovative visual method capable of mapping the potential flooding risk of each canal and ditch section, particularly useful for managing flood-prone areas. The risk segmentation provided by RCS has proven to be a powerful and flexible approach (tool) for decisionmakers, such as water planners, managers, as well as civil protection agencies, to anticipate potential impacts and improve the prevention and enable more effective flood management strategies tailored to local conditions. In this sense, RCS has made it possible to identify areas of special interest where flood-induced risk to irrigation infrastructure might negatively affect its operational capacity, as well as increase the hazard by transforming these infrastructures into elements of risk in themselves (as flow vectors). In this sense, hydraulic reality after a severe flooding event with or without linear infrastructures may be very different. In addition, this detailed visualization approach allows, on the one hand, to prioritize risk minimization actions in a more effective way, and, on the other hand, it can contribute to a better and easier understanding of flood phenomena and increase citizen awareness, in line with the EU Floods Directive objectives.

Author Contributions: J.-L.M., F.E., S.Z. and C.P.-A. conceived, designed, and led the research. All authors created the research conceptualization and analytical development. J.-L.M. supervised all actions. The Discussion and Conclusions sections were addressed by all authors, and all authors wrote the paper. All authors have read and agreed to the published version of the manuscript.

Funding: This research was funded by the Ministry of Science and Innovation, TED2021-129478BI00, through the Research Project "Intelligent and Digital System for the Ecological Restoration of Degraded Reservoirs (SID_REDES)", granted to the Research Group "INGENIERÍA Y GESTIÓN DEL AGUA (IGA)" of Salamanca University, Spain, and it has been developed within project "SOSTENIBILIDAD, AGUA Y AGRICULTURA EN EL SIGLO XXI" of the call for the Program "Misiones Ciencia e Innovación" for the year 2021 of Ministry of Science and Innovation, MIG-20211026. SOSTENIBILIDAD DE GRANDES EMBALSES MEDIANTE LA PREDICCION DE LA CAPACIDAD DE ALMACENAMIENTO (SOGECAL): PID2022-142299OB-I00.

Data Availability Statement: Data is contained within the article.

Acknowledgments: The authors thank the University of Salamanca for the facilities made available to undertake this research.

Conflicts of Interest: The authors declare no conflicts of interest. The funders had no role in the design of the study; in the collection, analyses, or interpretation of data; in the writing of the manuscript; or in the decision to publish the results.

References

1. Ogie, R.I.; Holderness, T.; Dunn, S.; Turpin, E. Assessing the vulnerability of hydrological infrastructure to flood damage in coastal cities of developing nations. *Comput. Environ. Urban Syst.* **2018**, *68*, 97–109. [CrossRef]
2. Arrighi, C.; Pregnolato, M.; Castelli, F. Indirect flood impacts and cascade risk across interdependent linear infrastructures. *Nat. Hazard. Earth Syst. Sci.* **2021**, *21*, 1955–1969. [CrossRef]
3. Valipour, M.; Krasilnikof, J.; Yannopoulos, S.; Kumar, R.; Deng, J.; Roccaro, P.; Mays, L.; Grismer, M.E.; Angelakis, A.N. The Evolution of Agricultural Drainage from the Earliest Times to the Present. *Sustainability* **2020**, *12*, 416. [CrossRef]
4. Chen, P. On the Diversity-Based Weighting Method for Risk Assessment and Decision-Making about Natural Hazards. *Entropy* **2019**, *21*, 269. [CrossRef]

5. Barros, V.R.; Field, C.B.; Dokke, D.J.; Mastrandrea, M.D.; Mach, K.J.; Bilir, T.E.; Chatterjee, M.; Ebi, K.L.; Estrada, Y.O.; Genova, R.C. *IPCC. Climate Change 2014: Impacts, Adaptation, and Vulnerability. Part B: Regional Aspects*; Contribution of Working Group II to the Fifth Assessment Report of the Intergovernmental Panel on Climate Change; Cambridge University Press: Cambridge, UK; New York, NY, USA, 2014.
6. Jongman, B.; Hochrainer-Stigler, S.; Feyen, L.; Aerts, J.C.J.H.; Mechler, R.; Wouter Botzen, W.J.; Bouwer, L.M.; Pflug, G.; Rojas, R.; Ward, P.J. Increasing stress on disaster-risk finance due to large floods. *Nat. Clim. Chang.* **2014**, *4*, 264–268. [CrossRef]
7. Zazo, S.; Rodríguez-Gonzálvez, P.; Molina, J.-L.; González-Aguilera, D.; Agudelo-Ruiz, C.; Hernández-López, D. Flood Hazard Assessment Supported by Reduced Cost Aerial Precision Photogrammetry. *Remote Sens.* **2018**, *10*, 1566. [CrossRef]
8. Insurance Compensation Consortium. Available online: https://www.consorseguros.es/web/documents/10184/44193/Estadistica_Riesgos_Extraordinarios_1971_2014/14ca6778-2081-4060-a86d-728d9a17c522 (accessed on 20 May 2023).
9. Kron, W. Flood Risk=Hazard•Values•Vulnerability. *Water Int.* **2005**, *30*, 58–68. [CrossRef]
10. Kappes, M.S.; Keiler, M.; von Elverfeldt, K.; Glade, T. Challenges of analyzing multi-hazard risk: A review. *Nat. Hazard.* **2012**, *64*, 1925–1958. [CrossRef]
11. Mladineo, N.; Mladineo, M.; Benvenuti, E.; Kekez, T.; Nikolić, Ž. Methodology for the Assessment of Multi-Hazard Risk in Urban Homogenous Zones. *Appl. Sci.* **2022**, *12*, 12843. [CrossRef]
12. Criado, M.; Martínez-Graña, A.; San Román, J.; Santos-Francés, F. Flood Risk Evaluation in Urban Spaces: The Study Case of Tormes River (Salamanca, Spain). *Int. J. Environ. Res. Public Health* **2018**, *16*, 5. [CrossRef] [PubMed]
13. Davoine, P.A.; Arnaud, A.; Gensel, J.; Martin, H. A tool for historical cartography about natural hazards. In Proceedings of the 22nd International Cartographic Conference, A Coruña, Spain, 9–16 July 2005.
14. Kellens, W.; Vanneuvile, W.; Ooms, K.; De Maeyer, P. Communicating flood risk to the public by cartography. In Proceedings of the 24th International Cartographic Conference, Santiago, Chile, 15–21 November 2009.
15. Ministerio Para la Transformación Ecológica y el Reto Demográfico. Available online: https://www.miteco.gob.es/es/agua/temas/gestion-de-los-riesgos-de-inundacion/guia-evaluacion-resiliencia-nucleos-urbanos-riesgo-inundacion_tcm30-503725.pdf (accessed on 10 April 2023).
16. Milanesi, L.; Pilotti, M.; Ranzi, R. A Conceptual Model of People's Vulnerability to Floods. *Water Resour. Res.* **2015**, *51*, 182–197. [CrossRef]
17. Zazo, S.; Molina, J.-L.; Macian-Sorribes, H.; Pulido-Velazquez, M. Assessment of the predictability of inflow to reservoirs through Bayesian Causality. *Hydrol. Sci. J.* **2023**, *68*, 1323–1337. [CrossRef]
18. Oliva Cañizares, A.; Sainz-Pardo Trujillo, A.; Sánchez Almodóvar, E. *La Cartografía de Vulnerabilidad Como Base de Los Planes de Emergencia: Análisis-Diagnóstico del Término Municipal de Daya Vieja (Alicante)*; University of Alicante: Alicante, Spain, 2020.
19. Abellán Contreras, F. *Medidas y Acciones Preventivas Contra Inundaciones en la Cuenca Del Segura: Una Perspectiva Histórico-Jurídica*; University of Alicante: Alicante, Spain, 2020.
20. Maurandi Guirado, A.; Romero Díaz, M.A. *Las Inundaciones en la Cuenca Del Segura en Las Dos Últimas Décadas Del Siglo xx. Actuaciones de Prevención*; Serie Geográfica; University of Alcala de Henares: Álcala de Henares, Spain, 2020; pp. 93–120.
21. Canales Martínez, G. *Avenamiento y Utilización de Aguas Muertas. La Cultura Del Agua en la Cuenca Del Segura (Murcia)*; Fundación Cajamurcia: Murcia, Spain, 2004; pp. 439–477.
22. Morato, J.V.B.G.; Oxinaga, P.I.M.; Abdilla, J.M. *Corredores Hidráulicos Verdes y Lagunas de Laminación en la Vega Baja Del Segura. Inundaciones y Sequías: Análisis Multidisciplinar Para Mitigar el Impacto de Los Fenómenos Climáticos Extremos*; University of Alicante: Alicante, Spain, 2021; pp. 471–492.
23. Brémond, P.; Grelot, F.; Agenais, A.L. Economic evaluation of flood damage to agriculture–review and analysis of existing methods. *Nat. Hazard. Earth Syst. Sci.* **2013**, *13*, 2493–2512. [CrossRef]
24. Cohen, A.N.; Fishhendler, I. An archetype for insurance thresholds for extreme natural events in the agricultural sector. *Clim. Risk Manag.* **2022**, *36*, 100434. [CrossRef]
25. Cronología de Riadas en la Cuenca Del Segura. Available online: https://www.chsegura.es/es/confederacion/unpocodehistoria/cronologia-de-riadas-en-la-cuenca-del-Segura (accessed on 22 May 2023).
26. Olcina-Cantos, J. *Inundaciones de Septiembre de 2019 en la Vega Baja Del Segura. La Oportunidad Del Plan "Vega Renhace"*; University of Alicante: Alicante, Spain, 2019.
27. Pedreño, J.; Lucas, I.G. *Los Servicios Ecosistémicos Del Suelo y su Papel en la Mitigación de Las Inundaciones*; University of Miguel Hernández : Elche, Spain, 2021.
28. Ojeda, A.O.; Ortiz, M.I.; Melgarejo, J. Crecidas, inundaciones y resiliencia: Restauración fluvial contra los falsos mitos. In *Riesgo de Inundación en España: Análisis y Soluciones Para la Generación de Territorios Resilientes*; University of Alicante: Alicante, Spain, 2020; pp. 549–568.
29. Olcina-Cantos, J.; Oliva Cañizares, A.; Sánchez Almodóvar, E.; Martí Talavera, J.; Biener Camacho, S. Cartografías para la acreditación del riesgo de inundaciones: SNCZI y PATRICOVA en la Comunidad Valenciana (España). *GeoFocus Rev. Int. Cienc. Tecnol. Inf. Geográfica* **2021**, *27*, 19–53. [CrossRef]
30. Agroseguro. Available online: https://agroseguro.es/wp-content/uploads/2022/10/Informe_Anual_2020.pdf (accessed on 23 May 2023).
31. Informe de Fundación AON España. Available online: https://fundacionaon.es/wp-content/uploads/2022/03/Informe-Coste-Catastrofes-Naturales-2016-2020.pdf (accessed on 23 April 2023).

32. Trapote, A.; Roca Roca, J.F.; Mejgarejo, J. *Azudes y Acueductos Del Sistema de Riego Tradicional de la Vega Baja Del Segura (Alicante, España)*; University of Alicante: Alicante, Spain, 2015.
33. Morote Seguido, Á.F.; Gómez Espín, J.M.; Hervás Avilés, R.M. *Patrimonio Hidráulico y Cultura Del Agua en el Mediterráneo. Murcia*; Investigaciones Geográficas: Fundación Séneca. Regional Campus of Excellence "Campus Mare Nostrum"; Agencia Española de Cooperación Internacional para el Desarrollo: Madrid, Spain, 2012; 287p.
34. PATRICOVA. Available online: https://visor.gva.es/visor/ (accessed on 25 May 2023).
35. Xia, K.; Wei, C. Study on Real-Time Navigation Data Model Based on ESRI Shapefile. In Proceedings of the International Conference on Embedded Software and Systems Symposia (ICESS), Chengdu, China, 29–31 July 2008.
36. Ritter, N.; Ruth, M. The GeoTiff data interchange standard for raster geographic images. *Int. J. Remote Sens.* **1997**, *18*, 1637–1647. [CrossRef]
37. Centro Nacional de Información Geográfica. Información Geográfica Temática. Available online: https://centrodedescargas.cnig.es/CentroDescargas/index.jsp (accessed on 24 April 2023).
38. Plan Nacional de Ortofotografía Aérea. Available online: https://pnoa.ign.es/web/portal/pnoa-lidar/especificaciones-tecnicas (accessed on 28 April 2023).
39. Graser, A.; Olaya, V. Processing: A Python Framework for the Seamless Integration of Geoprocessing Tools in QGIS. *ISPRS Int. J. Geo-Inf.* **2015**, *4*, 2219–2245. [CrossRef]
40. Ozgur, C.; Colliau, T.; Rogers, G.; Hughes, Z. MatLab vs. Python vs. R. *J. Data Sci.* **2021**, *15*, 355–372. [CrossRef]
41. Van Rossum, G.; Drake, F.L. *The Python Language Reference. Release 3.6.0*; Python Software Foundation: Wilmington, DE, USA, 2017; p. 157.
42. Lawhead, J. *QGIS Python Programming Cookbook*; Packt Publishing Ltd.: Birmingham, UK, 2015; p. 318.
43. Lemenkova, P.; Debeir, O. GDAL and PROJ Libraries Integrated with GRASS GIS for Terrain Modelling of the Georeferenced Raster Image. *Technologies* **2023**, *11*, 46. [CrossRef]
44. Willman, J. *Modern PyQt: Create GUI Applications for Project Management, Computer Vision, and Data Analysis*; Apress: Berkeley, CA, USA, 2021; pp. 1–42.
45. Cox, R.J.; Shand, T.D.; Blacka, M.J. Australian Rainfall and Runoff revision project 10: Appropriate safety criteria for people. *Water Res.* **2010**, *978*, 085825-9454.
46. IGA Ingeniería y Gestión del Agua (University of Salamanca, Ávila, Spain). *Proyecto: SOS-AGUA XXI: Sostenibilidad, Agua y Agricultura en el Siglo XXI*; Technical Report Task 1.5; University of Salamanca: Ávila, Spain, 2023.
47. Ranzi, R.; Mazzoleni, M.; Milanesi, L.; Pilotti, M.; Ferri, M.; Giuriato, F.; Mikoš, M. *Critical Review of Non-Structural Measures for Water-Related Risks*; KULTURisk: Delft, The Netherlands, 2011; p. 42.
48. Gil-Guirado, S.; Pérez-Morales, A.; Pino, D.; Peña, J.C.; Martínez, F.L. Flood impact on the Spanish Mediterranean coast since 1960 based on the prevailing synoptic patterns. *Sci. Total Environ.* **2022**, *807*, 150777. [CrossRef]
49. Vietz, G.J.; Rutherfurd, I.D.; Fletcher, T.D.; Walsh, C.J. Thinking outside the channel: Challenges and opportunities for protection and restoration of stream morphology in urbanizing catchments. *Landsc. Urban Plan.* **2016**, *145*, 34–44. [CrossRef]
50. Esteve, P.; Varela-Ortega, C.; Blanco-Gutiérrez, I.; Downing, T.E. A hydro-economic model for the assessment of climate change impacts and adaptation in irrigated agriculture. *Ecol. Econ.* **2015**, *120*, 49–58. [CrossRef]
51. Prenger-Berninghoff, K.; Cortes, V.J.; Sprague, T.; Aye, Z.C.; Greiving, S.; Głowacki, W.; Sterlacchini, S. The connection between long-term and short-term risk management strategies for flood and landslide hazards: Examples from land-use planning and emergency management in four European case studies. *Nat. Hazard. Earth Syst. Sci.* **2014**, *14*, 3261–3278. [CrossRef]